## DISCLAIMER

**This report was prepared as an account of work sponsored by an agency of the United States Government. Neither the United States Government nor any agency thereof, nor any of their employees, makes any warranty, express or implied, or assumes any legal liability or responsibility for the accuracy, completeness, or usefulness of any information, apparatus, product, or process disclosed, or represents that its use would not infringe privately owned rights. Reference herein to any specific commercial product, process, or service by trade name, trademark, manufacturer, or otherwise does not necessarily constitute or imply its endorsement, recommendation, or favoring by the United States Government or any agency thereof. The views and opinions of authors expressed herein do not necessarily state or reflect those of the United States Government or any agency thereof. Reference herein to any social initiative (including but not limited to Diversity, Equity, and Inclusion (DEI); Community Benefits Plans (CBP); Justice 40; etc.) is made by the Author independent of any current requirement by the United States Government and does not constitute or imply endorsement, recommendation, or support by the United States Government or any agency thereof.**

**SANDIA REPORT**
SAND2025-08617
Printed July 2025

Sandia National Laboratories

# Computational Prediction of Infrasound Arrival Times and Directions from Stationary and Moving Impulsive Sources

Elizabeth A. Silber

Prepared by
Sandia National Laboratories
Albuquerque, New Mexico
87185 and Livermore,
California 94550

Issued by Sandia National Laboratories, operated for the United States Department of Energy by National Technology & Engineering Solutions of Sandia, LLC.



Available to DOE and DOE contractors from
U.S. Department of Energy
Office of Scientific and Technical Information
P.O. Box 62
Oak Ridge, TN 37831

Telephone: (865) 576-8401
Facsimile: (865) 576-5728
E-Mail: reports@osti.gov
Online ordering: http://www.osti.gov/scitech

Available to the public from
U.S. Department of Commerce
National Technical Information Service
5301 Shawnee Rd
Alexandria, VA 22312

Telephone: (800) 553-6847
Facsimile: (703) 605-6900
E-Mail: orders@ntis.gov
Online order: https://classic.ntis.gov/help/order-methods/

## ABSTRACT

This report addresses the need to predict infrasound signal arrival times and back azimuths at monitoring stations, enabling more focused and efficient searches within recorded waveform data. The primary challenge is estimating expected signal arrival windows for stationary and moving acoustic sources, such as chemical explosions, volcanic eruptions, meteoroids, and spacecraft re-entry events. To address this challenge, a reproducible methodology is described that uses simplified propagation speeds for boundary layer, tropospheric, stratospheric, and thermospheric atmospheric waveguides. While the Python source code itself is not freely available, this document provides detailed, step-by-step instructions, and equations enabling users to replicate and adapt the method independently. The method reliably predicts signal arrival intervals and back azimuths, thereby supporting rapid detection and accurate interpretation of infrasound events. Results demonstrate that this method effectively identifies plausible signal arrival intervals and directions, facilitating faster event detection and more reliable interpretation. This methodology directly supports atmospheric monitoring, planetary defense, and forensic analysis of explosive atmospheric events.

## ACKNOWLEDGEMENTS

The author acknowledges support provided by the Sandia's Laboratory Directed Research & Development (LDRD) program, project number 229346.

## CONTENTS

## LIST OF FIGURES

## EXECUTIVE SUMMARY

Accurate detection and analysis of low-frequency acoustic signals (infrasound) are essential for identifying explosive atmospheric events, including chemical detonations, volcanic eruptions, meteorite impacts, and spacecraft re-entries. Reliable predictions of when and from which direction these signals will reach monitoring stations significantly improve the efficiency and effectiveness of data analysis. This report provides a detailed methodology designed to predict infrasound signal arrival times and directions (back azimuths) at monitoring stations. The method calculates signal arrival windows through four distinct atmospheric layers: boundary layer, troposphere, stratosphere, and thermosphere, and accounts separately for stationary events and moving events, the latter of which require calculations for multiple trajectory points. While the original computational Python code is not freely available, this report explains the underlying principles, equations, and computational steps, allowing users to independently replicate the predictive model. Implementation of this method reduces the effort required to search recorded waveform data, improving both the speed and accuracy of event detection. This methodology is broadly applicable to scientific research, environmental monitoring, and planetary defense operations.

This page left blank

## ACRONYMS AND TERMS

| Acronym/Term | Definition |
|---|---|
| CSV | comma-separated values |
| Hz | Hertz |
| ID | identifier |
| NASA | National Aeronautics and Space Administration |
| OSIRIS-REx | Origins, Spectral Interpretation, Resource Identification, and Security – Regolith Explorer |
| UTC | Coordinated Universal Time |

This page left blank

# 1. INTRODUCTION

This report presents a step-by-step overview of a computational algorithm designed to predict infrasound signal arrival windows and source directions (back azimuths). The algorithm serves as a first-line analytical tool, effectively narrowing waveform segments of interest and aiding in the detection of impulsive atmospheric events, such as bolides, explosions, and spacecraft re-entries. By systematically identifying expected arrival intervals and corresponding source directions, this method facilitates targeted waveform analysis, thereby reducing the scope and effort required for subsequent, more detailed propagation modeling.

Infrasound is defined as acoustic waves with frequencies below the lower threshold of human hearing, typically less than 20 Hz [1]. These low-frequency acoustic signals propagate efficiently through Earth's atmosphere, traveling over significant distances due to atmospheric waveguide ducting [2, 3]. Infrasound signals originate from a diverse range of natural and anthropogenic phenomena, including nuclear [4] and other explosions [5], volcanic eruptions [6], earthquakes [7], severe weather events [8], rocket launches [9], and bolides [10]. The latter results from meteoroids entering Earth's atmosphere at hypersonic velocities. Each of these phenomena generates infrasound signatures that vary in duration, amplitude, frequency content, and source characteristics.

For decades, infrasound has played an essential role in global monitoring systems designed to detect atmospheric and terrestrial explosive events [11, 12]. This role primarily included monitoring nuclear tests and other lower yield explosions, where the identification and location of such events have critical global security implications. Beyond these anthropogenic sources, infrasound has become increasingly valuable for scientific investigations of natural events. For instance, volcanic eruptions often produce infrasound signals that can be used for early warning and eruption monitoring. Severe atmospheric weather, such as tornadoes and thunderstorms, also emit infrasound signatures, enabling remote detection and analysis even when visual or radar observations are limited.

One particularly important application of infrasound monitoring is the detection and characterization of bolides [13]. Bolides present significant concern due to their potential threat to populated areas and infrastructure, illustrated by the 2013 Chelyabinsk airburst [14], and are of scientific interest for planetary defense efforts and assessing Earth's meteoroid influx rate [10, 15, 16]. Traveling at velocities ranging from 11.2 to 72.8 km/s, these extraterrestrial objects produce intense shock waves as they encounter Earth's atmosphere [17]. Similarly, spacecraft re-entries such as National Aeronautics and Space Administration's (NASA's) recent Origins, Spectral Interpretation, Resource Identification, and Security – Regolith Explorer (OSIRIS-REx) mission [18] generate substantial acoustic signatures along elongated atmospheric trajectories [19, 20]. Both types of events produce infrasonic signals that can propagate over hundreds or thousands of kilometers from their origin. Due to the intense physical conditions in the non-linear shock region, including extreme heating, rapid ablation, and often fragmentation [21], these sources generate acoustic signatures that can be distinctively more complex, both spatially and temporally, compared to signals from stationary explosive events [22].

Given the importance of accurately identifying and characterizing atmospheric events based on acoustic signals, estimating infrasound signal arrival time windows and directional bearings (back azimuths) at monitoring stations is essential [13, 23, 24]. Initial prediction of these arrival windows is critical for analysts, as it enables them to define and narrow search intervals within extensive waveform records, significantly reducing the time and effort required for effective detection and source identification [13]. To achieve this initial prediction, a computational approach utilizing distinct

atmospheric waveguides (the boundary layer, troposphere, stratosphere, and thermosphere) is employed. These waveguides represent typical acoustic propagation pathways, providing bounds on the earliest and latest possible arrival times [2] without relying on more detailed and computationally intensive numerical propagation modeling [25, 26]. The back azimuth is initially established based on direct line-of-sight calculations along great-circle paths, providing approximate source direction. This initial predictive capability lays the groundwork for subsequent, more detailed analyses that consider realistic atmospheric conditions. An illustrative example of complex infrasound propagation behavior, showing multiple atmospheric ray paths between a hypothetical source and a distant monitoring station, is given in Figure 1.

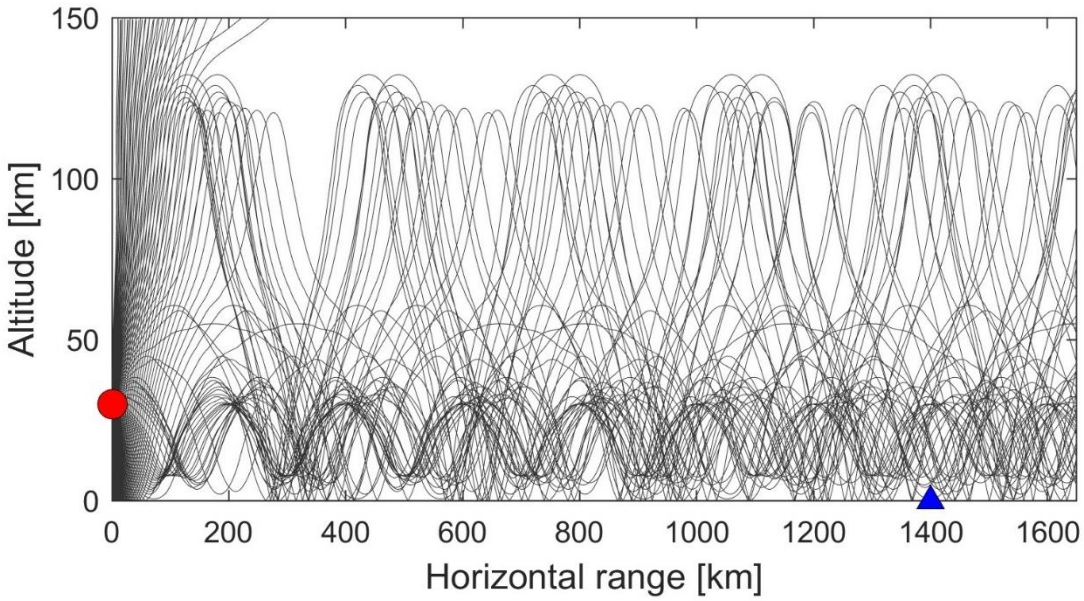


**Figure 1: Illustrative example showing modeled atmospheric propagation paths of infrasound signals originating from a hypothetical source at 30 km altitude (red circle). Acoustic energy propagates along multiple atmospheric pathways (ray paths), reflecting and refracting within atmospheric waveguides, before being detected by a ground-based monitoring station approximately 1400 km from the source (blue triangle). Such complex propagation behavior demonstrates the necessity of a systematic predictive method to estimate signal arrival windows and directions at distant stations.**

This report provides detailed methods and guidelines for estimating infrasound arrival windows and back azimuths for both stationary (fixed-location) and moving (trajectory-based) acoustic sources, emphasizing their application for global monitoring and scientific investigation. The ability to accurately predict these infrasound signal characteristics is essential not only for immediate event identification and response but also for improving the understanding of acoustic propagation through Earth's complex and dynamic atmosphere. While detailed computational modeling using numerical propagation models (such as ray tracing or parabolic equation methods) is accurate, it is also computationally expensive and time-consuming. Therefore, a first-order predictive approach is highly valuable, providing rapid estimates of expected arrival windows before analysts undertake more detailed and computationally demanding propagation modeling.

.

## 2. THEORETICAL BACKGROUND

Accurate and timely identification of atmospheric events based on their infrasonic signals depends critically on knowing when and from which direction signals are expected to arrive. Given known event coordinates (latitude, longitude) and event origin time, this method computes the earliest and latest plausible arrival times of acoustic signals at fixed monitoring stations, as well as an approximate direction of arrival (back azimuth).

### 2.1 Detection Probability Time Window

The great circle distance $d$ (in km) between a source and a monitoring station, represented as two latitude–longitude pairs ($\phi_1$, $\lambda_1$) and ($\phi_2$, $\lambda_2$) on Earth is given by the haversine formula [27]:

$$d = 2R\ \sin^{-1}\left[\sqrt{\sin^2\left(\frac{\phi_2-\phi_1}{2}\right) + \cos(\phi_1)\cos(\phi_2)\sin^2\left(\frac{\lambda_2-\lambda_1}{2}\right)}\right] \qquad (1),$$

where $R$ = 6,371 km is Earth's mean radius (as per World Geodetic System 84 (WGS84)[28]).

The average acoustic propagation speeds ($c_{avg}$) or celerities used to establish arrival windows correspond to four representative atmospheric waveguides [2, 3]:

- Boundary layer waveguide (surface to ~1 km altitude, $c_{avg}$ = 340 m/s and as fast as 350 m/s)
- Tropospheric waveguide (~1–15 km altitude, $c_{avg}$ = 330 m/s)
- Stratospheric waveguide (~20–50 km altitude, $c_{avg}$ = 280 m/s)
- Thermospheric waveguide (around 100 km altitude, $c_{avg}$ = 220 m/s, and as slow as 180 m/s)

The earliest plausible signal arrival time at a station is computed using the fastest celerity (350 m/s), and the latest plausible arrival time is computed using the slowest celerity (180 m/s). Thus, the predicted arrival window encompasses all potential arrivals:

- Earliest arrival ($T_{min}$): $T_0 + \frac{d}{350\ m/s}$;
- Latest arrival ($T_{max}$): $T_0 + \frac{d}{180\ m/s}$.

Here, $T_0$ is the event time. Intermediate arrivals corresponding to tropospheric and stratospheric waveguides fall within this predicted window.

### 2.2 Predicted Back Azimuth

In addition to arrival time predictions, estimating the signal's back azimuth, the direction from the station to the source, is critical. This estimate is obtained from spherical geometry as follows:

$$\alpha = \tan^{-1} 2\ [\sin(\lambda_2 - \lambda_1)\ \cos(\phi_2), \cos(\phi_1)\ \sin(\phi_2)\ -\ \sin(\phi_1)\ \cos(\phi_2)\ \cos(\lambda_2 - \lambda_1)] \qquad (2).$$

This computed back azimuth represents a direct, line-of-sight bearing along the great-circle path, providing a baseline direction that is useful as a first-order approximation. It does not initially account for atmospheric effects, particularly crosswinds, which may slightly alter the apparent direction of acoustic wave arrival at the station. Such deviations are typically addressed in subsequent, more detailed propagation analyses.

The predictive methodology outlined in this report provides an efficient initial assessment of potential arrival windows and directions, enabling rapid event detection and narrowing the search space for analysts before employing more comprehensive numerical atmospheric modeling techniques.

# 3. COMPUTATIONAL METHODOLOGY FOR STATIONARY SOURCES

A stationary acoustic source represents an event originating from a fixed geographic point, such as a chemical explosion, volcanic eruption, or a localized event. To predict infrasound arrival windows at distant monitoring stations, total travel time is computed using known celerity (effective propagation speed) ranges for acoustic signals within Earth's atmosphere. To bound all possible signal arrivals, arrival windows are explicitly calculated for each atmospheric waveguide: boundary layer (350–340 m/s), tropospheric (330 m/s), stratospheric (280 m/s), and thermospheric (220–180 m/s). These calculations provide realistic earliest and latest arrival scenarios for stationary sources. We define the maximum possible celerity as 350 m/s (fastest boundary-layer conditions) and the minimum celerity as 180 m/s (slowest thermospheric conditions), ensuring that all potential acoustic arrivals are bounded within this range.

- Step 1: Determine the great-circle distance between the stationary source and each monitoring station (as defined in Section 2, Eq. (1)).
- Step 2: Compute total travel times (in seconds) for highest and lowest possible celerities to establish the arrival window. The earliest arrival window is then $T_{\min}$ and the latest is $T_{\max}$ as defined in Section 2.
- Step 3: Calculate the back azimuth for directional guidance (as defined in Section 2, Eq. (2)).

## 3.1 Stationary Source Example

To illustrate the calculation of predicted infrasound arrival windows and back azimuths for a stationary acoustic source, we consider a hypothetical event located in near Niagara Falls (43.0828° N, 79.0742° W), observed from a monitoring station in Toronto (43.6532° N, 79.3832° W) (Figure 2). Assuming an event origin time of 2025-06-01 at 12:00:00 UTC, the great-circle distance, arrival window using the defined highest and lowest atmospheric acoustic celerities (350 m/s and 180 m/s, respectively), and the corresponding back azimuth from the station toward the source are calculated below.

- Event location: Niagara Falls (43.0828° N, 79.0742° W)
- Monitoring station: Toronto (43.6532° N, 79.3832° W)
- Event origin time: 2025-06-01 12:00:00 UTC
- Great-circle distance: 68.17 km
- Back azimuth: 158.40°
- Earliest arrival time (350 m/s celerity): 12:03:14.76 UTC (travel time: 194.76 seconds)
- Latest arrival time (180 m/s celerity): 12:06:18.70 UTC (travel time: 378.70 seconds)

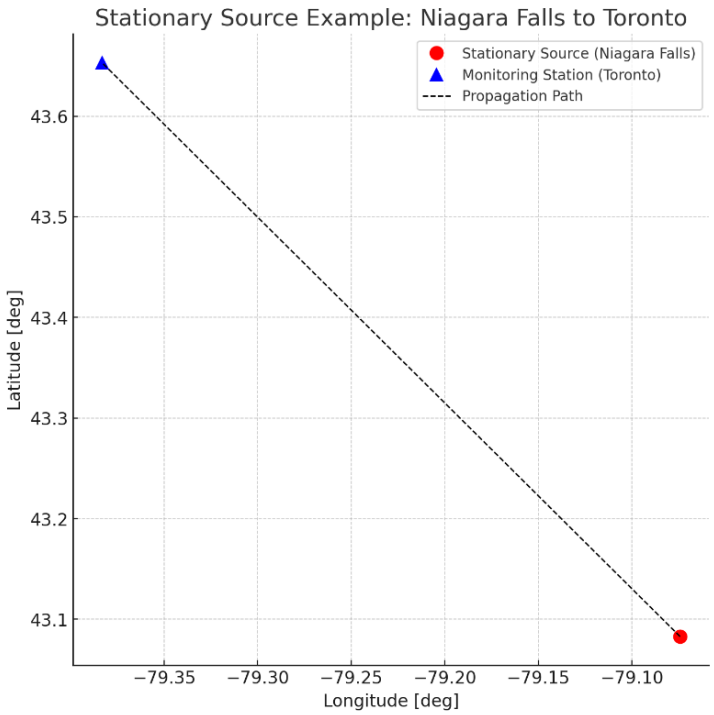


**Figure 2: A stationary source scenario, showing Niagara Falls as the stationary acoustic source (red circle), Toronto as the monitoring station (blue triangle), and the direct propagation path connecting them.**

# 4. COMPUTATIONAL METHODOLOGY FOR MOVING SOURCES

Moving acoustic sources, such as meteoroids [13], spacecraft re-entry capsules [19], and other objects traversing Earth's atmosphere at high speeds, might produce infrasonic signals along extended trajectories rather than at single fixed locations [29]. Because acoustic signals from these moving sources originate continuously along their atmospheric paths, calculating accurate arrival windows and back azimuth ranges at monitoring stations requires consideration of multiple points along their trajectory.

## 4.1 Importance of Trajectory Beginning and End Points

To accurately establish the overall arrival-time window and range of potential back azimuths, at least two primary points along the trajectory are identified: the trajectory's initial atmospheric entry point (begin point) and the final termination point (end point) [30]. The begin point represents the location where the source is expected to first produce detectable acoustic signals, typically at higher altitudes. The end point represents the location of the final expected significant acoustic emission (e.g., an airburst, fragmentation, or landing), typically at lower altitudes.

Using these two extremes ensures that the resulting predicted arrival-time window encompasses all potential signals emitted along the trajectory. This approach provides a practical and conservative prediction interval, helping analysts to narrow down the recorded waveform search intervals at monitoring stations efficiently.

## 4.2 Altitude Considerations

At close monitoring distances (tens to a few hundred kilometers), the altitude of acoustic emission points can become significant compared to horizontal ground distances [31]. Under these conditions, altitude differences can substantially influence the total acoustic travel distance, arrival times, and propagation geometry. As altitude directly contributes to the slant distance (the straight-line path between source and observer), failing to account for altitude differences at short ranges can introduce notable errors in the predicted arrival windows and back azimuths. Therefore, when the altitude of emission points is not negligible compared to the horizontal distance to the station, altitude must explicitly be included in distance calculations. At longer ranges (hundreds to thousands of kilometers), the relative effect of altitude generally becomes less significant compared to the overall propagation path.

## 4.3 Computational Steps

Step 1: Identify begin and end points of the trajectory
Establish the geographic coordinates (latitude and longitude) and if necessary, approximate altitude for both the initial entry and final termination points.

Step 2: Calculate great-circle distances
Separately calculate great-circle distances from both trajectory points (begin and end) to each monitoring station.

Step 3: Calculate total travel times using highest and lowest celerities
Moving sources require arrival windows explicitly calculated at each trajectory point (begin and end) for each atmospheric waveguide (boundary layer, tropospheric, stratospheric, and thermospheric). This approach ensures accurate and realistic prediction intervals for moving sources. We can start by

computing travel times for the highest possible celerity (350 m/s, representing the fastest propagation conditions, typically boundary layer) and the lowest possible celerity (180 m/s, representing the slowest propagation conditions, typically thermospheric) from each trajectory point to the station.

- Earliest possible arrival (fastest wave speed): the minimum of the arrival times calculated from both trajectory points using 350 m/s celerity.
- Latest possible arrival (slowest wave speed): the maximum of the arrival times calculated from both trajectory points using 180 m/s celerity.

Thus, the total predicted arrival window at any station is established between these two extremes.

Step 4: Calculate back azimuths
Compute the back azimuths separately from each trajectory point to the monitoring station. These two values define a directional span (minimum to maximum) from which acoustic signals may be expected, establishing the realistic range of signal arrival directions.

## 4.4 Moving Source Example

An example illustrating the calculation of predicted infrasound arrival windows and back azimuths for a moving acoustic source is presented here. We consider a hypothetical event traveling along a trajectory starting near Niagara Falls (43.0828° N, 79.0742° W) and terminating in the Toronto area (43.6532° N, 79.3832° W), with acoustic signals observed from a monitoring station in Ottawa (45.4215° N, 75.6994° W) (Figure 3). Assuming the event occurs at 2025-06-01 12:00:00 UTC, separate calculations are performed for both the initial and final trajectory points. The resulting great-circle distances, arrival times (using highest celerity of 350 m/s and lowest celerity of 180 m/s), and corresponding back azimuths establish the overall arrival window and directional span. This example illustrates how extended trajectories produce broader signal arrival intervals and back azimuth ranges, reflecting realistic acoustic propagation scenarios associated with moving atmospheric sources.

Trajectory initial point (Niagara Falls) to Ottawa:

- Distance: 373.93 km
- Fastest travel time (350 m/s): 1068.38 seconds (~17 min 48 s)
- Slowest travel time (180 m/s): 2077.41 seconds (~34 min 37 s)
- Back azimuth: 227.13°

Trajectory final point (Toronto) to Ottawa:

- Distance: 351.95 km
- Fastest travel time (350 m/s): 1005.58 seconds (~16 min 46 s)
- Slowest travel time (180 m/s): 1955.29 seconds (~32 min 35 s)
- Back Azimuth: 237.34°

Overall predicted arrival window at Ottawa:

- Earliest possible arrival: 2025-06-01 12:16:45 UTC (fastest arrival from Toronto)
- Latest possible arrival: 2025-06-01 12:34:37 UTC (slowest arrival from Niagara Falls)

Back azimuth range:

- From 227.13° (initial point near Niagara Falls) to 237.34° (final point near Toronto).

These results illustrate the necessity of using multiple points along a moving source trajectory to establish realistic predictions of arrival windows and back azimuth ranges, particularly when trajectory length and altitude differences significantly affect the predicted acoustic signal characteristics at close range.

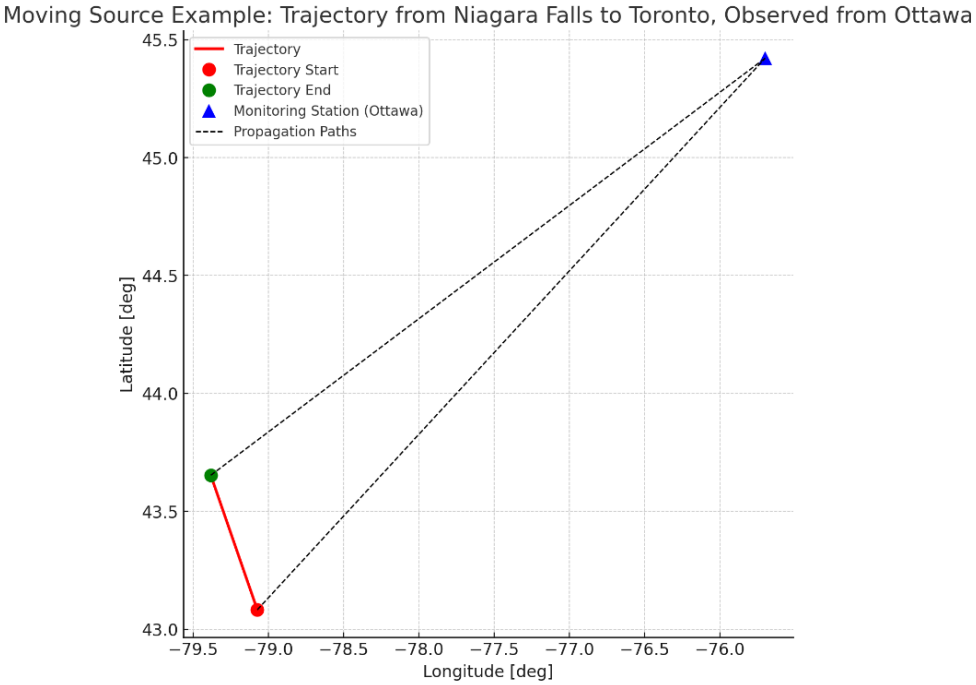


**Figure 3: The moving source scenario, showing the extended trajectory from Niagara Falls (trajectory start, red circle) to Toronto (trajectory end, green circle), with the monitoring station located in Ottawa (blue triangle). Dashed lines clearly represent the propagation paths from each end of the trajectory to Ottawa, highlighting the spatial extent and the range of expected back azimuths.**

# 5. PYTHON IMPLEMENTATION AND COMPUTATIONAL EXAMPLES

This section describes the computational approach used to implement the methodologies outlined in Sections 3 (stationary sources) and 4 (moving sources). The Python-based tool developed as part of this report enables users to perform systematic calculations of predicted infrasound arrival windows and back azimuths. The implementation supports various operational configurations, including single-source to single-station, single-source to multiple-stations, multiple-sources to single-station, and multiple-sources to multiple-stations. Users can modify input files to accommodate these scenarios according to their specific operational or research needs. The implementation leverages standard Python libraries, ensuring straightforward adaptation and broad compatibility across different computational environments.

The provided Python approach serves as one illustrative example among several possible computational implementations of this methodology. While the described algorithm and associated coding approach offer guidance and a structured framework, users are encouraged to adapt or implement alternative coding strategies as needed. Thus, the current implementation represents a guideline rather than a prescriptive or exclusive solution, accommodating flexibility in computational methods based on user preference and requirements.

## 5.1 Python Implementation Overview

The Python implementation requires structured input data provided in two separate comma-separated values (CSV) files. The first input file (stations.csv) contains geographic coordinates and identifiers for one or more monitoring stations. The second input file (sources.csv) lists one or more acoustic sources or events, including precise geographic coordinates and exact Coordinated Universal Time (UTC) event timestamps. These input files are designed to allow easy modification, thereby accommodating various combinations of source and station scenarios as required by the user's specific application or analysis.

The stations.csv file contains station identifiers (StationID) along with latitude and longitude coordinates for each station.

```
StationID,Latitude,Longitude
TOR,43.6532,-79.3832
OTT,45.4215,-75.6994
```

The sources.csv file includes detailed event identifiers (EventID), latitude and longitude coordinates, and the exact event date and time in separate columns (year, month, day, hour, minute, second). Proper formatting of these input files is important for successful execution and accurate computational results.

```
EventID,Latitude,Longitude,Year,Month,Day,Hour,Minute,Second
NF,43.0828,-79.0742,2025,6,1,12,0,0
TO,43.6532,-79.3832,2025,6,1,12,0,0
```

These files can be easily modified to represent various event and monitoring station scenarios as required.

## 5.2 Computational Procedure

The computational methodology involves multiple systematic steps executed by the Python implementation.

### *5.2.1 Great Circle Distance*

Initially, great-circle distances between each acoustic source and monitoring station are calculated using the haversine formula (Eq. (1)). This calculation provides spherical distances that form the basis for subsequent arrival time estimations.

```python
import math

def haversine_distance(lat1, lon1, lat2, lon2):
    R = 6371.0  # Earth's radius in kilometers
    lat1, lon1, lat2, lon2 = map(math.radians, [lat1, lon1, lat2, lon2])
    dlat = lat2 - lat1
    dlon = lon2 - lon1
    a = math.sin(dlat/2)**2 + math.cos(lat1) * math.cos(lat2) * math.sin(dlon/2)**2
    c = 2 * math.asin(math.sqrt(a))
    return R * c
```

### *5.2.2 Back Azimuth Calculation*

The next computational step determines the acoustic back azimuth from the monitoring station towards the acoustic source. The back azimuth calculation explicitly uses spherical geometry, ensuring accurate directional information critical for waveform data searches and analyses (Eq. (2)).

```python
def calculate_back_azimuth(sta_lat, sta_lon, src_lat, src_lon):
    sta_lat, sta_lon, src_lat, src_lon = map(math.radians, [sta_lat, sta_lon, src_lat, src_lon])
    dlon = src_lon - sta_lon
    x = math.sin(dlon) * math.cos(src_lat)
    y = math.cos(sta_lat) * math.sin(src_lat) - math.sin(sta_lat) * math.cos(src_lat) * math.cos(dlon)
    baz = (math.degrees(math.atan2(x, y)) + 360) % 360
    return baz
```

### 5.2.3 Arrival Time Computation

Subsequently, arrival windows for predicted acoustic signals are computed using predefined acoustic propagation celerities representing different atmospheric waveguides. The Python implementation explicitly includes calculations for the boundary layer (maximum and average celerities), tropospheric, stratospheric, and thermospheric waveguides (average and minimum celerities). These waveguides represent plausible acoustic propagation pathways within Earth's atmosphere, and their associated celerities ensure comprehensive coverage of potential arrival scenarios.

```python
from datetime import datetime, timedelta

waveguides = {
    'Boundary Layer (Max)': 350,
    'Boundary Layer (Avg)': 340,
    'Tropospheric': 330,
    'Stratospheric': 280,
    'Thermospheric (Avg)': 220,
    'Thermospheric (Min)': 180
}

def calculate_arrival_times(event_time, distance_km, waveguides):
    arrival_times = {}
    for name, speed in waveguides.items():
        travel_seconds = distance_km * 1000 / speed
        arrival = event_time + timedelta(seconds=travel_seconds)
        arrival_times[name] = {'Travel Time (s)': round(travel_seconds, 2),
                               'Arrival Time (UTC)': arrival.strftime('%Y-%m-%d %H:%M:%S')}
    return arrival_times
```

For stationary sources, the predicted arrival windows and back azimuths are computed directly from the single provided geographic event location. For moving sources, the methodology explicitly computes distances, back azimuths, and arrival times from at least two critical trajectory points (initial and final locations). This approach ensures comprehensive coverage of the full potential signal emission range along the object's trajectory.

## 5.3 Output and Data Interpretation

The Python implementation provides structured computational results in a well-organized CSV output file (predicted_infrasound_arrivals.csv). This output summarizes computed great-circle distances, back azimuths, total travel times (in seconds), and predicted arrival times (UTC) for each atmospheric waveguide scenario considered. The structured output facilitates straightforward integration with subsequent waveform analysis tasks, allowing analysts to efficiently narrow down their search intervals and clearly identify predicted signal directions.

The output CSV file contains defined columns such as EventID, StationID, Distance (km), Back Azimuth (deg), and travel times and arrival times for each waveguide. This structured format simplifies further analyses and provides a reliable foundation for more detailed acoustic propagation modeling, if required by subsequent investigations.

## 5.4 Computational Flow Overview

The computational method implemented by the Python tool follows a structured and systematic sequence of steps (Figure 4):

- Input data acquisition: Two input CSV files (*stations.csv* and *sources.csv*) are prepared and loaded into the Python environment. These files contain geographic coordinates and precise timing information for acoustic events and monitoring stations.

- Distance calculation: Great-circle distances between acoustic sources and monitoring stations are computed using the haversine formula. This step establishes accurate spherical distances that form the basis for arrival time estimation.

- Back azimuth calculation: Back azimuth angles, indicating the direction from each monitoring station toward each acoustic source, are calculated using spherical geometric relationships.

- Arrival window calculation: Predicted acoustic arrival windows are computed based on defined atmospheric propagation celerities. These include the boundary layer (maximum and average celerities), tropospheric, stratospheric, and thermospheric (average and minimum celerities) waveguides, ensuring comprehensive representation of realistic propagation scenarios.

- Output generation: Computed results, including distances, back azimuth angles, propagation travel times, and predicted arrival times for each waveguide, are compiled into a structured CSV output file (*predicted_infrasound_arrivals.csv*). The structured output supports subsequent waveform analysis and event characterization.

This structured computational approach supports reliable first-order predictions of infrasound signal characteristics, facilitating rapid event detection and efficient waveform analysis prior to more detailed numerical atmospheric modeling.

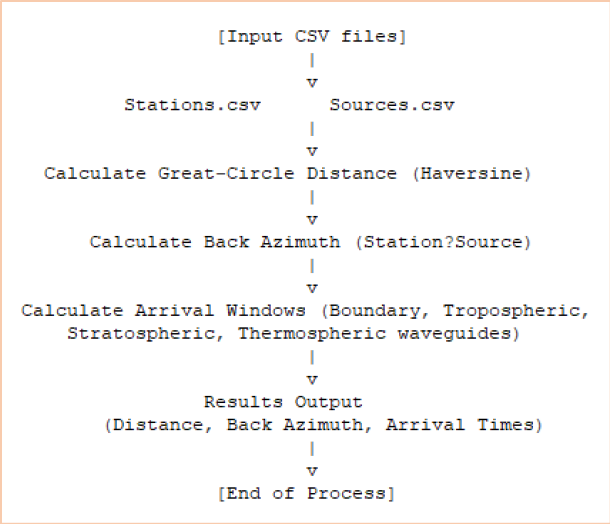


**Figure 4: Computational flow diagram.**

## 5.5 Optional Contextual Map Generation

Users can optionally extend the provided Python implementation to generate geographical maps illustrating event locations, station positions, trajectories (for moving sources), and great-circle propagation paths. Incorporating such visualizations may assist users in better understanding the geographical context of events and signal pathways, supporting improved situational awareness and interpretation. The recommended Python libraries for map generation include matplotlib and cartopy. Example scripts or existing templates can be readily modified to visualize input data and computed results effectively.

# 6. ADDITIONAL CONSIDERATIONS AND LIMITATIONS

The computational methodologies presented in this report provide first-order predictions suitable for initial event detection and analysis. However, certain limitations and considerations exist, including:

- Atmospheric conditions: This method employs simplified atmospheric propagation assumptions and does not directly consider atmospheric variability, such as temperature gradients, seasonal variations, or wind profiles. For rigorous analysis, detailed propagation modeling (e.g., ray tracing or parabolic equation methods) is recommended.
- Trajectory altitude impact: At short distances, variations in source altitude can significantly influence arrival times and signal detection, which should be carefully assessed, particularly when interpreting moving-source results.
- Crosswind effects on azimuth: Actual signal arrival directions (back azimuths) may differ slightly from line-of-sight predictions due to crosswinds and atmospheric refraction. These effects should be accounted for in more detailed analyses.

Users are encouraged to interpret the first-order computational predictions in conjunction with subsequent advanced modeling approaches to achieve comprehensive event characterization.

## 7. CONCLUSION

This report presents a robust computational methodology to predict infrasound signal arrival times and back azimuths at monitoring stations for both stationary and moving acoustic sources. The method provides reliable first-order estimation of expected signal arrival windows based on defined acoustic propagation celerities representative of various atmospheric waveguides. These calculations explicitly incorporate the boundary layer, tropospheric, stratospheric, and thermospheric propagation paths, establishing comprehensive bounds for plausible arrival times and directional bearings.

The accompanying Python-based implementation allows users to replicate the described computational approach and adapt it to various operational scenarios, including single-source/single-station, single-source/multiple-stations, multiple-sources/single-station, and multiple-sources/multiple-stations configurations. Additionally, the tool includes capabilities for optional contextual map generation, providing valuable visual interpretations of event locations, monitoring station positions, and predicted signal pathways.

While the approach facilitates efficient initial assessments and rapid event detection, detailed atmospheric modeling techniques are recommended for comprehensive analyses, particularly when considering complex atmospheric variability, including temperature gradients, seasonal variations, and wind profiles. Furthermore, the altitude of acoustic sources, especially in close-range scenarios involving moving sources, should be carefully accounted for to ensure accurate interpretations.

Overall, the computational methodology and provided Python implementation support rapid and reliable predictions of infrasound signal characteristics, effectively contributing to environmental monitoring, planetary defense, atmospheric research, and related operational applications.

This page left blank

## REFERENCES


[1] L. B. Evans, H. E. Bass, and L. C. Sutherland, "Atmospheric Absorption of Sound: Theoretical Predictions," *The Journal of the Acoustical Society of America,* vol. 51, no. 5B, pp. 1565-1575, 1972, doi: 10.1121/1.1913000.

[2] P. T. Negraru, P. Golden, and E. T. Herrin, "Infrasound Propagation in the "Zone of Silence"," *Seismological Research Letters,* vol. 81, no. 4, pp. 614-624, July 1, 2010 2010, doi: 10.1785/gssrl.81.4.614.

[3] P. T. Negraru and E. T. Herrin, "On Infrasound Waveguides and Dispersion," *Seismological Research Letters,* vol. 80, no. 4, pp. 565-571, July 1, 2009 2009, doi: 10.1785/gssrl.80.4.565.

[4] R. W. Whitaker, J. P. Mutschlecner, M. B. Davidson, and S. D. Noel, "Infrasonic observations of large scale HE events," LA-UR-90-1998; CONF-9005236--1, 1990. [Online]. Available: http://www.osti.gov/bridge/product.biblio.jsp?osti_id=7049095

[5] E. A. Silber, D. C. Bowman, and M. Ronac Giannone, "Detection of the Large Surface Explosion Coupling Experiment by a sparse network of balloon-borne infrasound sensors," *Remote Sensing,* vol. 15, no. 2, p. 542, 2023, doi: 10.3390/rs15020542.

[6] R. Matoza, D. Fee, D. Green, and P. Mialle, "Volcano infrasound and the international monitoring system," in *Infrasound monitoring for atmospheric studies*: Springer, 2019, pp. 1023-1077.

[7] S. Arrowsmith *et al.*, "Infrasound Signal Characteristics from Small Earthquakes," presented at the 2011 Monitoring Research Review: Ground-Based Nuclear Explosion Monitoring Technologies, Tuscon, AZ, 13-15 September 2011, 2011.

[8] J. D. Assink, L. G. Evers, I. Holleman, and H. Paulssen, "Characterization of infrasound from lightning," *Geophysical Research Lettters,* vol. 35, no. L15802, pp. 1-5, 2008, doi: 10.1029/2008GL034193.

[9] C. Pilger, P. Hupe, P. Gaebler, and L. Ceranna, "1001 Rocket Launches for Space Missions and Their Infrasonic Signature," *Geophysical Research Letters,* 10.1029/2020GL092262 vol. 48, no. 8, p. e2020GL092262, 2021/04/28 2021, doi: 10.1029/2020GL092262.

[10] E. A. Silber, "The utility of infrasound in global monitoring of extraterrestrial impacts: A case study of the 23 July 2008 Tajikistan bolide," *The Astronomical Journal,* vol. 168, no. 17, 2024, doi: 10.3847/1538-3881/ad47c3.

[11] N. Brachet, D. Brown, R. Bras, Y. Cansi, P. Mialle, and J. Coyne, "Monitoring the Earth's Atmosphere with the Global IMS Infrasound Network," in *Infrasound Monitoring for Atmospheric Studies*, A. Le Pichon, E. Blanc, and A. Hauchecorne Eds.: Springer Netherlands, 2010, pp. 77-118.

[12] D. R. Christie and P. Campus, "The IMS infrasound network: design and establishment of infrasound stations," in *Infrasound monitoring for atmospheric studies*: Springer, 2010, pp. 29-75.

[13] E. A. Silber, "Perspectives and Challenges in Bolide Infrasound Processing and Interpretation: A Focused Review with Case Studies," *Remote Sensing,* vol. 16, no. 19, p. 3628, 2024, doi: 10.3390/rs16193628.

[14] P. G. Brown *et al.*, "A 500-kiloton airburst over Chelyabinsk and an enhanced hazard from small impactors," *Nature,* Letter vol. 503, no. 7475, pp. 238-241, 2013, doi: 10.1038/nature12741.

[15] E. A. Silber, D. O. ReVelle, P. G. Brown, and W. N. Edwards, "An estimate of the terrestrial influx of large meteoroids from infrasonic measurements," *J. Geophys. Res.,* vol. 114, no. E8, p. E08006, 2009, doi: 10.1029/2009je003334.

[16] P. Brown, R. E. Spalding, D. O. ReVelle, E. Tagliaferri, and S. P. Worden, "The flux of small near-Earth objects colliding with the Earth," *Nature,* vol. 420, pp. 294-296, 2002, doi: 10.1038/nature01238.
[17] Z. Ceplecha *et al.*, "Meteor Phenomena and Bodies," *Space Science Reviews,* vol. 84, no. 3, pp. 327-471, 1998, doi: 10.1023/A:1005069928850.
[18] D. Lauretta *et al.*, "OSIRIS-REx: sample return from asteroid (101955) Bennu," *Space Science Reviews,* vol. 212, pp. 925-984, 2017.
[19] E. Silber and D. C. Bowman, "Along-trajectory acoustic signal variations observed during the hypersonic reentry of the OSIRIS-REx Sample Return Capsule," *Seismological Research Letters,* 2025, doi: 10.1785/0220250014.
[20] E. A. Silber *et al.*, "Geophysical Observations of the 24 September 2023 OSIRIS-REx Sample Return Capsule Re-Entry," *The Planetary Science Journal,* vol. 5, no. 9, 2024, doi: 10.3847/PSJ/ad5b5e.
[21] E. A. Silber, M. Boslough, W. K. Hocking, M. Gritsevich, and R. W. Whitaker, "Physics of meteor generated shock waves in the Earth's atmosphere – A review," *Advances in Space Research,* vol. 62, no. 3, pp. 489-532, 2018/08/01/ 2018, doi: 10.1016/j.asr.2018.05.010.
[22] T. C. Wilson, E. A. Silber, T. A. Colston, B. R. Elbing, and T. R. Edwards, "Bolide infrasound signal morphology and yield estimates: A case study of two events detected by a dense acoustic sensor network," *The Astronomical Journal,* vol. 169, no. 4, 2025, doi: 10.3847/1538-3881/adbb70.
[23] W. N. Edwards, P. G. Brown, and D. O. ReVelle, "Estimates of meteoroid kinetic energies from observations of infrasonic airwaves," *Journal of Atmospheric and Solar-Terrestrial Physics,* vol. 68, no. 10, pp. 1136-1160, 2006, doi: 10.1016/j.jastp.2006.02.010.
[24] T. A. Ens, P. G. Brown, W. N. Edwards, and E. A. Silber, "Infrasound production by bolides: A global statistical study," *Journal of Atmospheric and Solar-Terrestrial Physics,* vol. 80, pp. 208-229, 2012, doi: 10.1016/j.jastp.2012.01.018.
[25] C. de Groot-Hedlin, "Modeling Infrasound Waveforms in a Windy Environment," *Inframatics,* no. 11, pp. 2-7, 2005.
[26] *GeoAc: Numerical tools to model acoustic propagation in the geometric limit*. (2014). Los Alamos National Laboratory.
[27] R. W. Sinnott, "Virtues of the Haversine," *Sky and telescope,* vol. 68, no. 2, p. 158, 1984.
[28] U. S. D. M. A. USDMA, "Department of Defense World Geodetic System 1984: Its definition and relationships with local geodetic systems," Defense Mapping Agency, Fairfax, VA, 1991, vol. 8350.
[29] E. A. Silber, "Investigating the relationship between bolide entry angle and apparent direction of infrasound signal arrivals," *Pure and Applied Geophysics,* 2025, doi: 10.1007/s00024-025-03706-1.
[30] E. A. Silber, "Observational and theoretical investigation of cylindrical line source blast theory using meteors," PhD Thesis, Physics and Astronomy, Western University, London, ON, Canada, 2014.
[31] E. A. Silber and P. G. Brown, "Optical observations of meteors generating infrasound—I: Acoustic signal identification and phenomenology," *Journal of Atmospheric and Solar-Terrestrial Physics,* vol. 119, pp. 116-128, 2014, doi: 10.1016/j.jastp.2014.07.005.

## DISTRIBUTION

**Email—Internal**

| Name | Org. | Sandia Email Address |
|---|---|---|
| Daniel Gonzales | 6752 | dgonza2@sandia.gov |
| Technical Library | 1911 | sanddocs@sandia.gov |

This page left blank


Sandia National Laboratories is a multimission laboratory managed and operated by National Technology & Engineering Solutions of Sandia LLC, a wholly owned subsidiary of Honeywell International Inc. for the U.S. Department of Energy's National Nuclear Security Administration under contract DE-NA0003525.